

## Screening and identification of antioxidant active ingredients from red wine via spectrum-effect relationship analysis

Yuye Gao<sup>1,†</sup>, Xie-an Yu<sup>2,†</sup>, Bing Wang<sup>2</sup>, Yibao Jin<sup>2</sup>, Guo Yin<sup>2</sup>, Jue Wang<sup>2</sup>, Yi Lu<sup>2</sup>, Tiejie Wang<sup>1,2</sup>, Kaishun Bi<sup>1\*</sup>

<sup>1</sup>School of Pharmacy, Shenyang Pharmaceutical University, Shenyang, Liaoning, China; <sup>2</sup>NMPA Key Laboratory for Quality Research and Evaluation of Traditional Chinese Medicine, Shenzhen Institute for Drug Control, Shenzhen, China

<sup>†</sup>These authors contributed equally.

\*Corresponding author: Kaishun Bi, School of Pharmacy, Shenyang Pharmaceutical University, Shenyang, Liaoning, China. Email: [kaishunbi.syphu@gmail.com](mailto:kaishunbi.syphu@gmail.com)

Received: 17 February 2022; Accepted: 5 May 2022; Published: 1 January 2023

© 2023 Codon Publications

OPEN ACCESS



ORIGINAL ARTICLE

### Abstract

Red wine was a prominent constituent of diets across the globe and modern pharmacological studies showed that red wine had the main function of antioxidant. However, the reported screening methods for active ingredients were inefficient and insensitive. In this research, 35 batches of red wine were used to establish the chromatography fingerprint, which were further utilized to screen and identify the antioxidant active ingredients through spectrum-effect relationship analysis. Indeed, the antioxidant capacity of red wine was evaluated by total antioxidant capacity assay kit (ABTS method). After evaluating the antioxidant capacity of samples, correlations were analyzed by Pearson correlation analysis, Spearman correlation analysis, and Gray Relational Analysis (GRA). Moreover, spectrum-effect relationships combined with ultrafast liquid chromatography/quadrupole-time-of-flight mass spectrometry (UFLC-Q-TOF/MS) revealed that the succinic acid, gallic acid, protocatechuic acid, catechin, syringic acid, salicylic acid, homogentisic acid, ellagic acid, isorhamnetin-3-O-glucoside, and trans-resveratrol show antioxidative efficacy. Collectively, the present study established the spectrum-effect relationship strategy of red wine and identified active antioxidant ingredients, which would give reasonable index components for the health function of red wine and provide reference for quick screening of bioactive compounds for food.

**Keywords:** antioxidant activity; red wine; spectrum-effect relationship; UFLC-Q-TOF/MS

### Introduction

Wine is the product of the complete or partial fermentation of fresh grapes, or a mixture of that product and products derived solely from grapes, and a fermented wine with a certain degree of alcohol (Australia New Zealand Food Standards Code, 2004). Wine is classified by color into red wine, white wine, rose wine, and so on. Red wine showed higher antioxidant capacity compared with other type of wines (Fernández-Pachón *et al.*, 2006). Polyphenol was the main bioactive compound in wine, including phenolic acids and flavonoids such as succinic acid, gallic acid, protocatechuic acid, catechin, syringic

acid, salicylic acid, homogentisic acid, ellagic acid, trans-resveratrol, and isorhamnetin-3-O-glucoside, which shows antioxidant, anticoagulant, and lipid-lowering activities (Gao *et al.*, 2021; Haunschild Robin and Marx Werner, 2022). Antioxidant activity was one of the most important biological activities of red wine; therefore, it is important to explore the specific antioxidant activity from red wine.

The spectrum-effect relationship was a subject that established the internal relationship between fingerprint and biochemical detection by multiple data processing methods, which was used to evaluate the internal quality

(Rao *et al.*, 2022; Zhang *et al.*, 2018). Chromatography fingerprint had been internationally recognized as a feasible and reasonable quality evaluation method for traditional Chinese medicine, food and their related products with multi-components (Esteki *et al.*, 2019). World Health Organization (WHO) (Guidelines for the assessment of herbal medicines, 1991) and US Food and Drug Administration (FDA) (Botanical Drug Development Guidance for Industry, 2016) have included and promoted chromatographic fingerprint as the reliable method for the quality control (Chen *et al.*, 2019; Yang *et al.*, 2016). Some studies have shown that suitable intake of red wine can reduce oxidative stress damage caused by free radicals (Navajas-Porras *et al.*, 2020; Plumb *et al.*, 2020). Therefore, antioxidant capacity was frequently used to evaluate the intrinsic quality of red wine (Eke *et al.*, 2021). Currently, *in vitro* antioxidant screening methods are frequently used due to their high-throughput and low-cost characteristics (El-Demerdash Fatma *et al.*, 2021). Among these methods, the stable solid-free radical 2,2'-azino-bis (3-ethylbenzothiazoline-6-sulfonic acid) (ABTS) was employed in the assessment of antioxidant activity. During the relationship analysis, correlation analysis was a statistical method used to calculate correlation coefficient, which can reflect the order of contribution for each chromatographic fingerprint peak component to activity. Some studies have developed the relationship between chromatographic fingerprint and antioxidant activity, which could provide not only a method for screening active ingredients but also a comprehensive strategy for quality evaluation (Du *et al.*, 2021; Xu *et al.*, 2022). Accordingly, the spectrum-effect relationship could be used for quick screening of the potential active ingredients from complex samples.

To further elucidate the material basis of the antioxidant effect from red wine, 35 batches of red wine were used to establish the ultra-high-performance liquid chromatography (UHPLC) fingerprint and the antioxidant activity of them was also evaluated through total antioxidant capacity assay kit with ABTS method. Then, the correlation between common peaks and the result of antioxidant activity was calculated by Pearson correlation analysis, Spearman correlation analysis, and Gray Relational Analysis (GRA). Following the results of spectrum-effect relationships and ultrafast liquid chromatography/quadrupole-time-of-flight mass spectrometry (UFLC-Q-TOF/MS), succinic acid, gallic acid, protocatechuic acid, catechin, syringic acid, salicylic acid, homogentisic acid, ellagic acid, isorhamnetin-3-O-glucoside, and trans-resveratrol with the principally antioxidative substances were successfully screened. Hence, the present study established the spectrum-effect relationship strategy of red wine and identified active antioxidant ingredients, which would provide reference for quick screening of bioactive compounds from complex samples.

## Materials and Methods

### Reagents and chemicals

HPLC-grade acetonitrile (ACN) and methanol (MeOH) were purchased from Merck (Darmstadt, Germany). Trifluoroacetic acid (TFA) was obtained from Guangzhou Chemical Reagent Factory (Guangzhou, China). The water used in this study was purified by a Milli-Q water purification system (MA, USA). A total of 35 batches of red wine samples were collected from four countries, which included three grape varieties (Table 1). Total antioxidant capacity assay kit (ABTS) was purchased from Beyotime, Shanghai, China.

### Sample preparation

The red wine was analyzed immediately after it was opened. All red wine samples (2 mL) were filtrated through a 0.22 µm polyvinylidene fluoride membranes. All the samples were stored at 4°C in the dark prior to analysis.

### UHPLC chromatographic analysis

The UHPLC analysis was performed by an UltiMate 3000 RSLCnano UltiMate 3000 RSLCnano System liquid chromatograph (Thermo Technologies, MA, USA) equipped with a Dionex UltiMate 3000 pump, a Dionex UltiMate 3000 autosampler, and a Dionex UltiMate 3000 diode array detector. The chromatographic separation of red wine was achieved on an ACQUITY UPLC column (HSS T3, 1.8 µm, 2.1 × 100 mm, Waters, Ireland) at 30°C. The mobile phase was composed of water containing 0.1% TFA (A) and methanol (B) at a flow rate of 0.30 mL/min. The fingerprint elution program was conducted as follows: 0–15 min at 0–6% B, 15–20 min at 6–11% B, 20–30 min at 1–11% B, 30–45 min at 11–20% B, 45–55 min at 20–30% B, and 55–60 min at 30–90% B. The sample injection volume was 2 µL and the total run time for analysis was 60 min. The DAD wavelength was 220 nm.

### Similarity analysis

All chromatographic data of 35 batches of samples were exported as \*.AIA file from UHPLC. Similarity analysis (SA) was performed on those files by using "Similarity Evaluation System for Chromatographic Fingerprint of Traditional Chinese Medicine" software (Version 2004A, Chinese Pharmacopoeia Committee). S1 was set as the reference fingerprint, and a new control fingerprint (R) was generated after multi-point correction and automatic matching, then the similarity values of these

Table 1. Origin and varietal of the red wines tested.

Samples	Cultivar(s)	Location
S1	Cabernet Sauvignon	Maipo Valley, Chile (33°27'S; 70°40'W)
S2	Cabernet Sauvignon	The Central Valley of Chile (33°27'S; 70°40'W)
S3	Cabernet Sauvignon	Maipo Valley, Chile (33°27'S; 70°40'W)
S4	Cabernet Sauvignon	Maipo Valley and Aconcagua Valley, Chile (33°27'S; 70°40'W and 32°29'S; 70°01'W)
S5	Cabernet Sauvignon	Aconcagua Valley, Chile (32°29'S; 70°01'W)
S6	Cabernet Sauvignon	Mendoza, Argentina (32°53'S; 68°51'W)
S7	Cabernet Sauvignon	Mendoza, Argentina (32°53'S; 68°51'W)
S8	Cabernet Sauvignon	Mendoza, Argentina (32°53'S; 68°51'W)
S9	Cabernet Sauvignon	Mendoza, Argentina (32°53'S; 68°51'W)
S10	Cabernet Sauvignon	Mendoza, Argentina (32°53'S; 68°51'W)
S11	Cabernet Sauvignon	Clare Valley, Australia (33°50'S; 138°36'E)
S12	Cabernet Sauvignon	Limestone Coast, Australia (30°20'S; 135°93'E)
S13	Cabernet Sauvignon	South Australia (33°40'S; 135°80'E)
S14	Cabernet Sauvignon	South Australia (33°40'S; 135°80'E)
S15	Cabernet Sauvignon	Clare Valley, Australia (33°50'S; 138°36'E)
S16	Cabernet Sauvignon	Changyu Vineyard, China (37°45'N; 121°43'E)
S17	Cabernet Sauvignon	Ganchengzi District, Qingtongxia, Ningxia, China (38°01'N; 106°04'E)
S18	Cabernet Sauvignon	Ningxia Helan Mountain East Foot Production Area, China (38°33'N; 106°20'E)
S19	Cabernet Sauvignon	Changyu Vineyard, China (37°45'N; 121°43'E)
S20	Cabernet Sauvignon	Changyu Vineyard, China (37°45'N; 121°43'E)
S21	Shiraz	Limestone Coast of Australia (30°20'S; 135°93'E)
S22	Shiraz	Great West, Australia (34°22'S; 117°60'E)
S23	Shiraz	Hunter Valley, Australia (33°30'S; 151°40'E)
S24	Shiraz	South Australia (33°40'S; 135°80'E)
S25	Shiraz	Barossa, Australia (34°30'S; 137°80'E)
S26	Shiraz	Pertway, Australia (36°50'S; 140°70'E)
S27	Shiraz	Kunawala, Australia (36°40'S; 140°50'E)
S28	Shiraz	Moray Valley, Chile (35°14'S; 71°27'W)
S29	Shiraz	Espinal Vineyard, Chile (33°27'S; 70°40'W)
S30	Shiraz	Pascual Toso, Argentina (32°53'S; 68°51'W)
S31	Merlot	Cachabel Valley, Chile (33°89'S; 71°45'W)
S32	Merlot	Curisco Valley, Chile (35°12'S; 71°31'W)
S33	Merlot	Konggagua Valley, Chile (34°90'S; 71°50'W)
S34	Merlot	Southeast Australia (33°40'S; 135°80'E)
S35	Merlot	Southeast Australia (33°40'S; 135°80'E)

samples were calculated. In addition, the common peaks in UHPLC fingerprints were observed.

### Antioxidant activity assay

The antioxidant activity of red wine was exhibited to restrict the absorbance of free radical cation ABTS, which showed a characteristic long-wavelength absorption spectrum with a maximum at 734 nm. The ABTS

radical was formed through a reaction with an oxidizing agent. Initially, 0.4 mL ABTS stock solution was mixed with 0.4 mL of the oxidizing agent solution for the preparation of the radical. This solution was maintained at room temperature for 12–16 h in an amber bottle. Subsequently, the mixture was diluted in phosphate-buffered saline (PBS) to obtain an absorbance of approximately  $0.7 \pm 0.05$ . Finally, different batches of red wine (10  $\mu$ L) were added and the absorbance of all test tubes was determined at 734 nm (Spagnol *et al.*, 2019).

## Statistical analysis

The correlation analysis was conducted between the common peak areas and activity data of red wine by statistical analysis of the GRA, Pearson correlation coefficient, and Spearman correlation coefficient. SPSS 24.0 (International Business Machines Corporation, New York, USA) was used to process the data and find common peaks that were significantly related to pharmacological effects.

## Mass spectrometry

The identification was performed on a hybrid quadrupole time-of-flight tandem mass spectrometry, UFLC-Q-TOF/MS (X500R QTOF, AB SCIEX, Foster City, CA) equipped with an electrospray ionization (ESI) interface. The mass spectrometer was operated in the negative ion mode. The following parameter settings were used: the ion spray voltage of 7 eV, turbo spray temperature (TEM) of 550°C, declustering potential (DP) of −100 V, collision energy (CE) of −45 V, nebulizer gas (gas 1) of 55 psi, heater gas (gas 2) of 55 psi, and curtain gas of 35 psi. Nitrogen was kept as the nebulizer and auxiliary gas. TOF-MS and TOF-MS/MS were scanned with the mass range of  $m/z$  100–1500 Da and 50–1500 Da, respectively. The experiments were run with 150 ms accumulation time for TOF MS and 50 ms accumulation time for TOF-MS/MS. Continuous recalibration was carried out at each five samples. In addition, dynamic background subtraction (DBS) trigger information-dependent acquisition (IDA) was used to trigger acquisition of MS/MS of low-level constituents. The accurate mass and composition for the precursor ions and fragment ions were analyzed using the SCIEX OS software integrated with the instrument.

## Results and Discussion

### Optimization of the chromatographic conditions

In order to obtain useful chemical information and better separation, several parameters including mobile phase composition, detection wavelength, and column temperature were carefully inspected as these parameters could positively influence the separation. The types and proportions of acid in the mobile phase were investigated. The conditions of adding 0.05% formic acid, 0.05% trifluoroacetic acid, 0.05% acetic acid, and pure water were also tested. As a result, 0.05% trifluoroacetic acid was better (Figure 1A). The conditions of adding 0.03% trifluoroacetic acid, 0.05% trifluoroacetic acid, and 0.1% trifluoroacetic acid in water were compared. The result showed that 0.1% trifluoroacetic acid was better (Figure 1B). The detection wavelength was tested at 210, 220, 254, and 280 nm. Under the wavelength of 220 nm, it was found

that more detectable common peaks, larger response values, and smoother baseline could be observed (Figure 1C). The column temperatures of 25°C, 30°C, and 35°C were evaluated. The result showed that the peak separation at 30°C was better (Figure 1D). The optimization of the chromatographic conditions is shown in Figure 1 and the fingerprint spectrum is shown in Figure 2.

### Methodology validation

The analytical method was validated for precision, repeatability, and stability. In precision testing, six consecutive injections of one sample solution were performed on the same day. Precision of peak area (PA) and retention time (RT) of 41 common peaks did not exceed 5.61% and 1.82% in relative standard deviation (RSD), respectively. Six independent samples were extracted and determined in parallel for the evaluation of repeatability. The RSD of peak area and RT of 41 common peaks was less than 5.99% and 1.77%. The stability was assessed by repeatedly analyzing one sample solution after being placed at room temperature for 0, 2, 4, 8, 12, and 24 h. The RSD of PA and RT of 41 common peaks was less than 5.70% and 1.72%, respectively. These results indicated that the established UHPLC fingerprint method for red wine was stable and reliable.

### UHPLC fingerprints of red wine and similarity evaluation

The fingerprints of 35 batches red wine were analyzed by similarity evaluation system. The values of similarity of generated reference fingerprint and sample fingerprints were calculated by similarity evaluation system. As a result, 41 common peaks were observed in UHPLC fingerprints (Figure 3). In Table 2, the similarity values between generated reference fingerprint and sample fingerprint were in the range of 0.445–0.972. According to the similarity evaluation system of chromatographic fingerprint of traditional Chinese medicine, the similarity between 0.9 and 1.0 was considered to meet the similarity requirement. These results demonstrated that there were differences between these samples. It was possible that the relative retention time (RT) or relative peak area (PA) of some peaks of red wine were not stably expressed, which might affect the antioxidant activity of red wine.

### Results of antioxidant activity

Antioxidant activity was one of the reasons why red wine was interested in food field. In this research, the antioxidant capacity of red wine was analyzed by ABTS scavenging assay and expressed as  $IC_{50}$ .  $IC_{50}$  was inversely proportional to the antioxidant capacity of red wine. Thirty-five batches of red wine were diluted to 5, 10, 20,



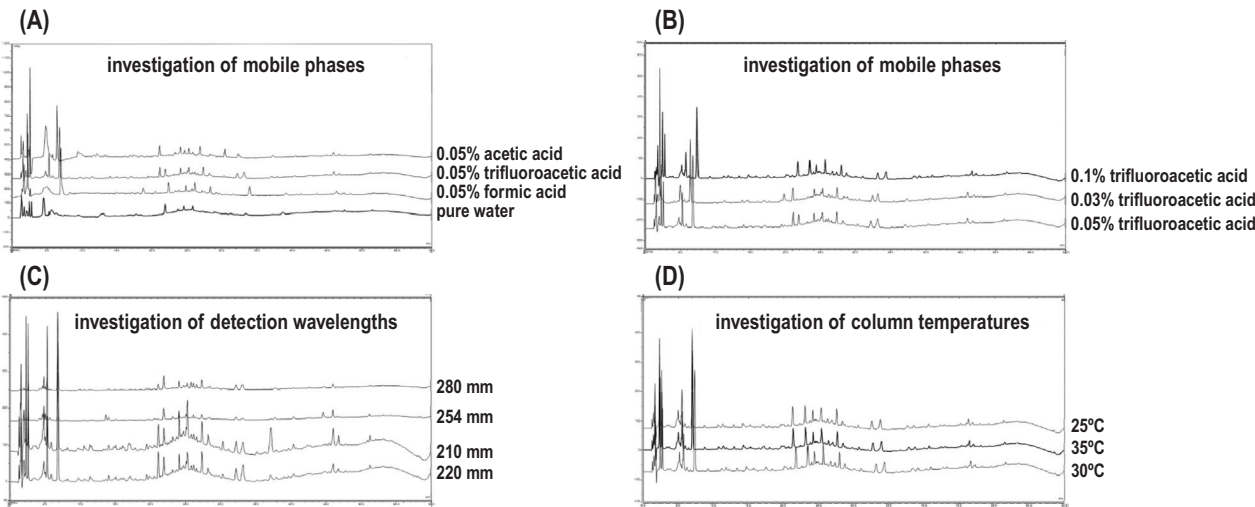


Figure 1. The optimization of the chromatographic conditions.

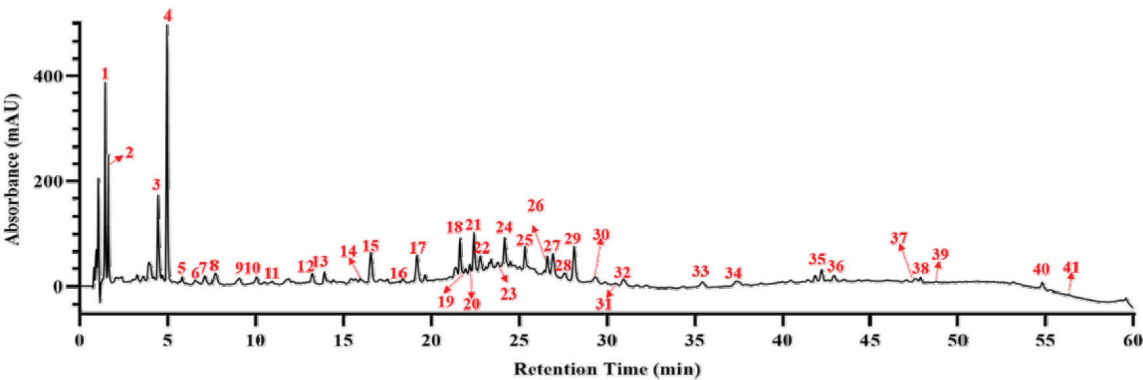


Figure 2. UHPLC fingerprint chromatogram of red wine.

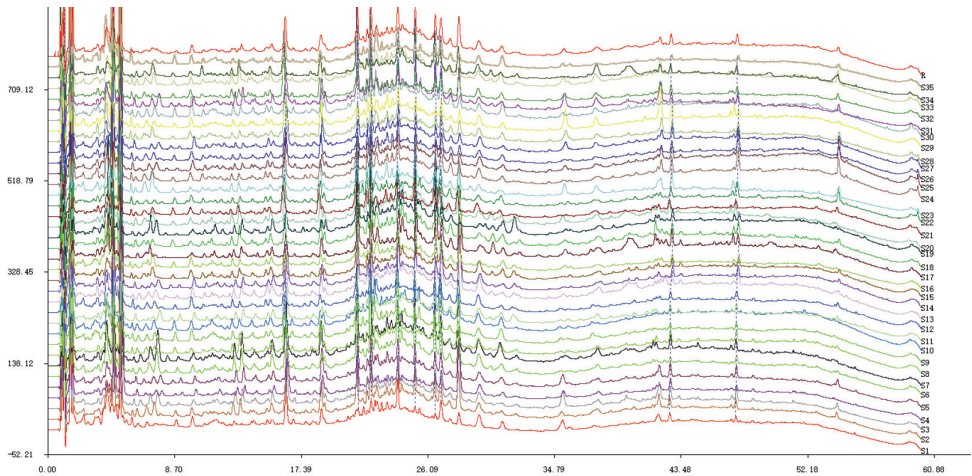


Figure 3. UHPLC fingerprints of different red wine samples.

**Table 2.** Similarity evaluation of 35 batches of red wine samples.

Sample No.	Similarity	Sample No.	Similarity
S1	0.886	S19	0.754
S2	0.916	S20	0.848
S3	0.824	S21	0.912
S4	0.870	S22	0.940
S5	0.914	S23	0.775
S6	0.959	S24	0.913
S7	0.812	S25	0.905
S8	0.936	S26	0.935
S9	0.936	S27	0.871
S10	0.947	S28	0.821
S11	0.946	S29	0.836
S12	0.934	S30	0.901
S13	0.920	S31	0.852
S14	0.946	S32	0.928
S15	0.972	S33	0.890
S16	0.445	S34	0.504
S17	0.863	S35	0.767
S18	0.918		

50, 100, 200, and 400 times to evaluate the antioxidant activity. The result is shown in Figure 4. The  $IC_{50}$  values of antioxidant activity for ABTS were in the range of 52.66–114.4 times of dilution times, hence a higher  $IC_{50}$  of dilution times showed a stronger antioxidant capacity. The results given in Table 3 show that red wine has good antioxidant activity.

### Results of correlation analysis

Correlation analysis can reflect the degree of correlation between variables. GRA, Pearson correlation, and Spearman correlation were used to examine the correlation of each peak and antioxidant activity directly; the closer the relationship between variables, the larger the absolute value of the correlation coefficient. The results of GRA show that the correlation coefficient from high to low as follows: P21 > P25 > P4 > P27 > P1 > P24 > P10 > P3 > P39 > P29 > P9 > P23 > P6 > P19 > P11 > P22 > P33 > P36 > P3 > P28 > P16 > P18 > P15 > P13 > P31 > P7 > P12 > P38 > P8 > P17 > P20 > P26 > P32 > P14 > P30. The larger correlation coefficients of P21, P25, P4, P27, P1, P24, and P10 of GRA were more than 0.95 suggesting that these seven peaks were closely related to antioxidant activity. The results of Pearson coefficient values were P24 > P25 > P27 > P38 > P39 > P29 > P21 > P33. Similarly, the results of Spearman coefficient values were P10 > P38 > P39 > P33 (Table 4). In the Pearson and Spearman correlation analysis, the correlations of P24, P25, P27,

P38, P39, P29, P21, P33, and P10 were significant at the 0.05 level, P39 and P33 were significant at the 0.01 level, which show that these nine components play key roles in the antioxidant activity of red wine. Taken together, integrated the three correlation analysis methods via the correlation coefficient (>0.95) of GRA and  $P$  value (<0.05) of Pearson correlation coefficient and Spearman correlation coefficient. Thus, P4, P10, P21, P24, P38, P1, P25, P27, P29, P39, and P33 were selected as potential antioxidant active ingredients, which when increased in concentration may enhance the antioxidant effect of red wine. Furthermore, the red wine was analyzed by UFLC-Q-TOF/MS and the chemical structures for 10 of the 11 screened compounds were identified.

### UFLC-Q-TOF/MS analyses of red wine

According to the result of three correlation analysis methods (GRA, Pearson, and Spearman correlation coefficient) as explained in the previous section, the peaks P1, P4, P10, P21, P24, P25, P27, P29, P33, P38, and P39 were selected as potential antioxidant active ingredients. The potential active compounds were identified by UFLC-Q-TOF/MS. The peak number, retention time, MS/MS fragmentation ions information, and identification of 10 components are listed in Table 5. The total ion chromatography is shown in Figure 5. Peak 1 has the major first-order mass spectrum at  $m/z$  117.0194 ( $C_4H_6O_4$ )  $[M-H]^-$ . The MS/MS fragments are at 99.0094 ( $C_3H_6O_3$ )  $[M-H-H_2O]^-$  and 73.0292 ( $C_4H_4O_3$ )  $[M-H-CO_2]^-$ . Therefore, it is identified as succinic acid (Huang *et al.*, 2012). Peak 4 shows the mass spectrum ion at  $m/z$  169.0141 ( $C_7H_6O_5$ )  $[M-H]^-$  and the product ion at 125.0247 ( $C_6H_6O_3$ )  $[M-H-CO_2]^-$  is also observed. As a result, it is identified as gallic acid (Gao *et al.*, 2021). Peak 10 has a molecular weight of 153.1092 ( $C_7H_6O_4$ ) with a fragment of 109.0296 ( $C_6H_6O_2$ )  $[M-H-CO_2]^-$ , and it is identified as protocatechuic acid (Ma *et al.*, 2015). Peak 21 has an  $[M-H]^-$  ion at  $m/z$  289.0715 ( $C_{15}H_{14}O_6$ ), the MS/MS fragmentation ions are at 245.0849 ( $C_{13}H_{14}O_4$ )  $[M-H-CO_2]^-$  and 203.0706 ( $C_{10}H_{12}O_3$ )  $[M-H-C_3H_2O_3]^-$ , which is identified as catechin (Svoboda *et al.*, 2015). Peak 24 shows the mass spectrum ion at  $m/z$  197.0456 ( $C_9H_{10}O_5$ )  $[M-H]^-$ , the product ion at 123.0077  $[M-H-2CH_3-CO_2]^-$  ( $C_6H_4O_3$ ) is supported to surmise it as syringic acid (Gao *et al.*, 2021). Peak 27 and Peak 29 have the major ions at  $m/z$  137.0244  $[M-H]^-$  ( $C_7H_6O_3$ ) and 167.0351  $[M-H]^-$  ( $C_8H_8O_4$ ), both have missed a  $CO_2$  fragment, the MS/MS fragments are at 93.0345  $[M-H-CO_2]^-$  ( $C_6H_6O$ ) and 123.0450  $[M-H-CO_2]^-$  ( $C_7H_8O_2$ ). Peak 29 has the other MS/MS fragment at 81.0352  $[M-H-CO_2-C_2H_2O]^-$  ( $C_5H_5O$ ), which is identified as salicylic acid and homogentisic acid (Gao *et al.*, 2021). Peak 33 shows the mass spectrum ion at 300.9987  $[M-H]^-$  ( $C_{14}H_6O_8$ ), the product fragment ions at 257.0110  $[M-H-CO_2]^-$  ( $C_{13}H_6O_6$ ) and 229.0126

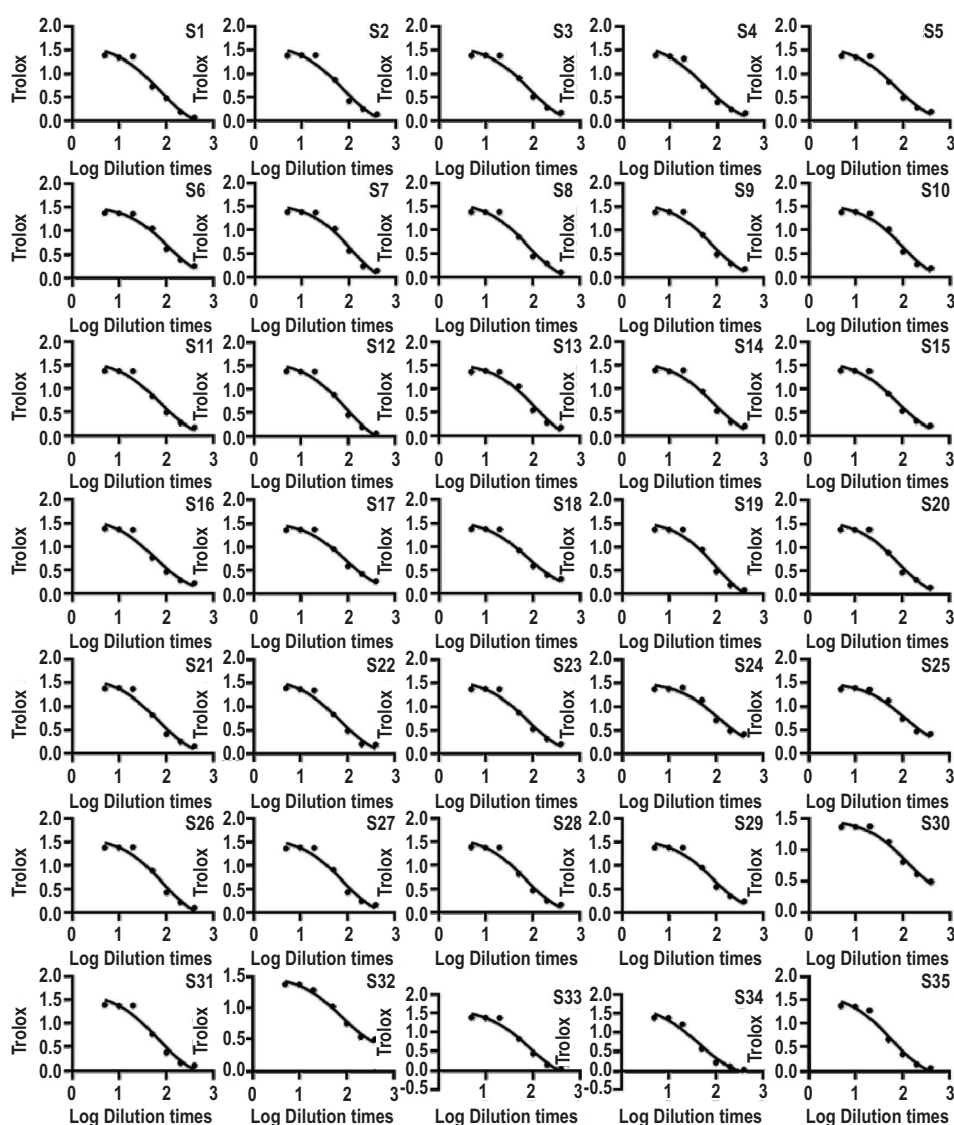


Figure 4. Determination of antioxidant activity of 35 batches of red wine.

[M-H-CO<sub>2</sub>-CO]<sup>-</sup> (C<sub>12</sub>H<sub>6</sub>O<sub>5</sub>), constituting the structure of ellagic acid (Yan *et al.*, 2014). Peak 38 has an [M-H]<sup>-</sup> ion at m/z 477.1044 (C<sub>22</sub>H<sub>22</sub>O<sub>12</sub>), the MS/MS fragmentation ions are at 315.0519 (C<sub>16</sub>H<sub>12</sub>O<sub>7</sub>) [M-H-C<sub>6</sub>H<sub>10</sub>O<sub>5</sub>]<sup>-</sup>, 271.0258 (C<sub>14</sub>H<sub>8</sub>O<sub>6</sub>) [M-H-C<sub>6</sub>H<sub>11</sub>O<sub>5</sub>-CH<sub>2</sub>-CHO]<sup>-</sup>, and 243.0308 (C<sub>13</sub>H<sub>8</sub>O<sub>5</sub>) [M-H-C<sub>6</sub>H<sub>11</sub>O<sub>5</sub>-CH<sub>2</sub>-CHO-CO]<sup>-</sup>, which is identified as isorhamnetin-3-O-glucoside (Tkacz *et al.*, 2020). Peak 39 has the major ions at m/z 227.0717 [M-H]<sup>-</sup> (C<sub>14</sub>H<sub>12</sub>O<sub>3</sub>) and the MS/MS fragment at 143.0496 [M-H-2C<sub>2</sub>H<sub>2</sub>O]<sup>-</sup> (C<sub>10</sub>H<sub>6</sub>O). Therefore, it is identified as trans-resveratrol (Bai *et al.*, 2021). Peak 25 is not identified by current qualitative analysis methods.

The identified compounds are polyphenols, which were reported many times for their antioxidant activity, anticoagulant activity, and so on (Gao *et al.*, 2021; Wang *et al.*, 2022). Gallic acid increases the antioxidant

enzyme activity and inhibits oxidative stress through a nuclear factor erythroid-2/nuclear factor kappa B-dependent (Nrf2/NF-κB-dependent) mechanism. In addition, gallic acid inhibits oxidative stress by increasing the expression of heme oxygenase-1 (HO-1) and Nrf2 genes, activating the signaling pathway of Nrf2/HO-1, decreasing the expression of NF-κB, inhibiting NF-κB pathway, and exerting anti-inflammatory effects (Sohrabi *et al.*, 2021). Protocatechuic acid plays an antioxidant role by increasing catalase and superoxide dismutase levels, reduces the level of glutathione and malondialdehyde (Albarakati, 2022). Syringic acid, salicylic acid, and ellagic acid exert the antioxidant capacity by activating Nrf2 (Lavigne *et al.*, 2022; Somade *et al.*, 2022; Zhang *et al.*, 2022). Isorhamnetin-3-O-glucoside significantly increases the level of glutathione (GSH) and the expression level of antioxidant enzymes

(including superoxide dismutase (SOD), catalase, glutathione reductase, and HO-1), preventing reactive oxygen species (ROS) induced cell damage (Kong *et al.*, 2009). Trans-resveratrol inhibits the levels of m-RNA of inflammatory markers NF- $\kappa$ B and tumor necrosis factor  $\alpha$  (TNF- $\alpha$ ), reduces the concentration of creatine kinase

(CK-MB), lactate dehydrogenase (LDH), and alkaline phosphatase, increases the concentration of superoxide dismutase and catalase, which plays an antioxidant role (Manjunatha *et al.*, 2020). Catechins can repair oxidative damage at a certain degree to some extent by regulating the activity of key enzymes related to GSH pathway (Zhao *et al.*, 2022). Some experiments showed that succinic acid and homogentisic acid have antioxidant activity (Al Khatib Maher *et al.*, 2021; Zarubina *et al.*, 2012), but the anti-oxidation mechanism has not been found. Therefore, comparison of our results to other researches shows that the screened compounds certainly have the antioxidant activity.

Table 3. The  $IC_{50}$  value of red wine samples.

Sample	$IC_{50}$	Sample	$IC_{50}$
S1	68.23	S19	93.1
S2	70.88	S20	77.03
S3	79.89	S21	63.38
S4	52.66	S22	66.25
S5	67.99	S23	74.33
S6	102.1	S24	110.7
S7	106.0	S25	109.3
S8	74.18	S26	78.14
S9	75.98	S27	73.71
S10	92.8	S28	65.74
S11	68.37	S29	80.9
S12	81.9	S30	114.4
S13	102.4	S31	59.05
S14	79.80	S32	73.71
S15	72.87	S33	74.22
S16	54.67	S34	38.82
S17	84.4	S35	50.29
S18	71.72		

### Confirmation of the antioxidant activity of the standards

In order to demonstrate the antioxidant capacity of the screened compounds, the antioxidant activity of the nine standards was determined. The antioxidant capacity of standards was analyzed by ABTS scavenging assay and expressed as  $IC_{50}$ . The standards were formulated as reserve fluids. Gallic acid (990  $\mu$ g/mL), protocatechuic acid (1005  $\mu$ g/mL), catechin (502.5  $\mu$ g/mL), syringic acid (1025  $\mu$ g/mL), salicylic acid (1004  $\mu$ g/mL), homogentisic acid (1025  $\mu$ g/mL), ellagic acid (980  $\mu$ g/mL), isorhamnetin-3-O-glucoside (495  $\mu$ g/mL), and isorhamnetin-3-O-glucoside (992  $\mu$ g/mL) were diluted to 1, 2, 4, 8, 16, 32, 64, 128, 256, and 512 times to evaluate the antioxidant activity. The results showed that the screened compounds and selected compounds have antioxidant activity. The  $IC_{50}$

Table 4. The results of GRA, Pearson, and Spearman correlation coefficient.

GRA		Pearson correlation coefficient			Spearman correlation coefficient		
Peak no.	Correlation Coefficient	Peak no.		TEAC	Peak no.		TEAC
21	0.961	10	Correlation Coefficient	0.406*	24	Correlation Coefficient	0.359*
25	0.96		P value	0.015		P value	0.034
4	0.959	38	Correlation Coefficient	0.364*	25	Correlation Coefficient	0.391*
27	0.957		P value	0.031		P value	0.02
1	0.954	39	Correlation Coefficient	0.467**	27	Correlation Coefficient	0.391*
24	0.953		P value	0.005		P value	0.02
10	0.951	33	Correlation Coefficient	0.450**	38	Correlation Coefficient	0.356*
-	-		P value	0.007		P value	0.036
-	-	-	-	-	39	Correlation Coefficient	0.454**
-	-	-	-	-		P value	0.006
-	-	-	-	-	29	Correlation Coefficient	0.411*
-	-	-	-	-		P value	0.014
-	-	-	-	-	21	Correlation Coefficient	0.357*
-	-	-	-	-		P value	0.035
-	-	-	-	-	33	Correlation Coefficient	0.403*
-	-	-	-	-		P value	0.017

\*  $P < 0.05$ ; \*\*  $P < 0.01$ .



Table 5. UFLC-Q-TOF/MS data and identification of 11 compounds with antioxidant activity from red wine.

Peak no.	RT (min)	[M-H] <sup>-</sup>	MS/MS fragmentation ions	Formula	Identification	ppm
1	1.38	117.0194	99.0094, 73.0292	C <sub>4</sub> H <sub>6</sub> O <sub>4</sub>	Succinic acid	-1.2
4	5.92	169.0141	125.0247	C <sub>7</sub> H <sub>6</sub> O <sub>5</sub>	Gallic acid	-1.0
10	11.72	153.0192	109.0296	C <sub>7</sub> H <sub>6</sub> O <sub>4</sub>	Protocatechuic acid	0.3
21	20.34	289.0715	245.0849, 203.0706, 123.0457, 109.0303	C <sub>15</sub> H <sub>14</sub> O <sub>6</sub>	Catechin	-1.5
24	22.06	197.0456	123.0077, 95.0134	C <sub>9</sub> H <sub>10</sub> O <sub>5</sub>	Syringic acid	-0.3
27	29.06	137.0244	93.0345	C <sub>7</sub> H <sub>6</sub> O <sub>3</sub>	Salicylic acid	1.0
29	30.67	167.0351	123.0450, 83.0137, 81.0352	C <sub>8</sub> H <sub>8</sub> O <sub>4</sub>	Homogentisic acid	0.8
33	38.70	300.9987	257.0110, 229.0126	C <sub>14</sub> H <sub>6</sub> O <sub>8</sub>	Ellagic acid	-0.9
38	45.61	477.1044	315.0519, 271.0258, 243.0308	C <sub>22</sub> H <sub>22</sub> O <sub>12</sub>	Isorhamnetin-3- O-glucoside	0.6
39	47.17	227.0717	143.0496	C <sub>14</sub> H <sub>12</sub> O <sub>3</sub>	Trans-resveratrol	0.6

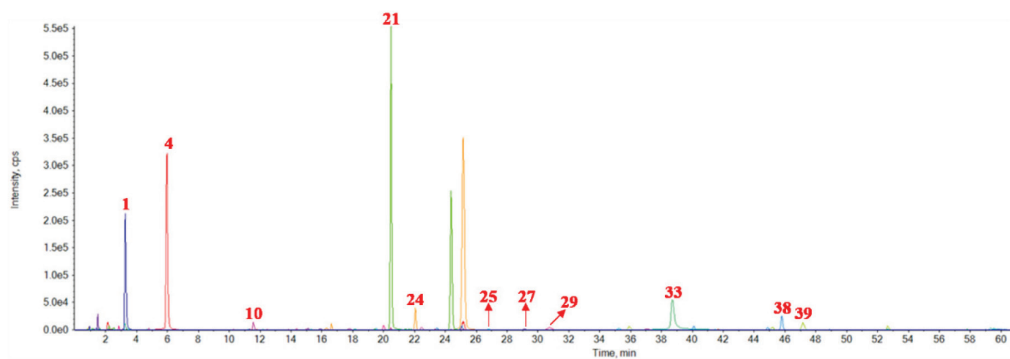


Figure 5. UFLC-Q-TOF/MS chromatography in a negative mode.

values are displayed in Figure 6 and the results are given in Table 6. An external experiment verified the result of correlation analysis.

### Conclusions

In this study, the antioxidant components of red wine were analyzed and partially identified using spectrum-effect relationship strategy and UFLC-Q-TOF/MS. The fingerprint of 35 batches were obtained using UHPLC and 41 common peaks were chosen through similarity analysis. Combined with the results of the ABTS assays, the spectrum-effect relationship was carried out to screen the active compounds. The results showed that the peaks with antioxidant components were P21, P24, P10, P38, P4, P27, P1, P39, P29, and P33, respectively. Finally, these peaks were identified as succinic acid, gallic acid, protocatechuic acid, catechin, syringic acid, salicylic acid, homogentisic acid, ellagic acid, isorhamnetin-3-O-glucoside, and trans-resveratrol through UFLC-Q-TOF/MS. Accordingly, the spectrum-effect relationship strategy was established and screened the antioxidant components from red wine, which could be used for quick screening of bioactive compounds from complex samples.

### Author contributions

Conceptualization, Kaishun Bi; data collection and methodology, Yuye Gao, Xie-an Yu, Bing Wang, Yibao Jin, Guo Yin, Jue Wang, and Yi Lu; data analysis, Yuye Gao and Xie-an Yu; writing—original draft preparation, Yuye Gao and Xie-an Yu; writing—review and editing, Tiejie Wang and Kaishun Bi. All authors have read and agreed to the published version of the manuscript.

### Acknowledgments

The authors would like to thank all the companions who selflessly supported this work.

### Funding

This research was funded by National Natural Science Foundation of China (No. 82104357) and Shenzhen Science and Technology Program (No. JCYJ20210324130408021).

### Conflicts of interest

The authors declare no conflicts of interest.

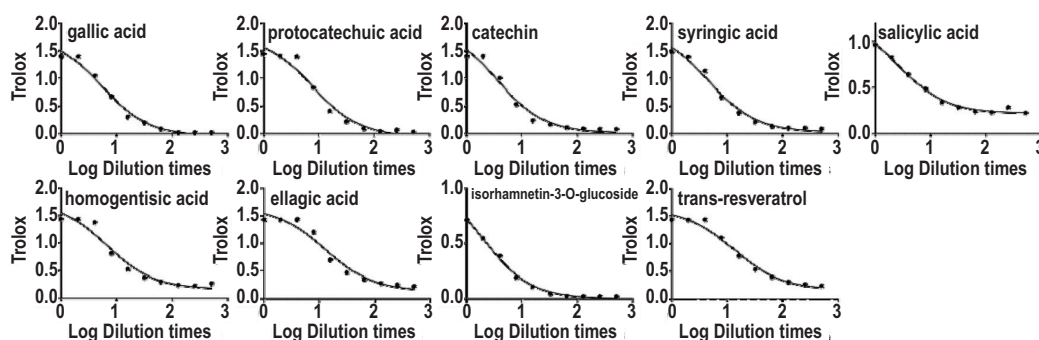


Figure 6. Determination of antioxidant activity of standards.

Table 6. The  $IC_{50}$  value of standards.

Standards	$IC_{50}$ ( $\mu$ g/mL)
Gallic acid	188.71
Protocatechuic acid	129.84
Catechin	141.55
Syringic acid	222.97
Salicylic acid	383.79
Homogentisic acid	158.94
Ellagic acid	76.26
Isorhamnetin-3-O-glucoside	248.99
Trans-resveratrol	75.38

## References

- Albarakati Alaa Jameel A. Protocatechuic acid counteracts oxidative stress and inflammation in carrageenan-induced paw edema in mice. *Environ Sci Pollut Res Int.* 2022 Aug;29(37):56393-56402. <https://doi.org/10.1007/s11356-022-19688-9>
- Al Khatib Maher, Costa Jessica, Spinelli Daniele, Capecci Eliana, Saladino Raffaele, Baratto Maria Camilla, *et al.* Homogentisic acid and gentisic acid biosynthesized pyromelanin mimics: Structural characterization and antioxidant activity. *Int J Mol Sci.* 2021;22(4):1739. <https://doi.org/10.3390/ijms22041739>
- Australia New Zealand Food Standards Code - Standard 4.5.1 - Wine Production Requirements (Australia Only), <https://www.legislation.gov.au/Details/F2011C00249>; 2004 [Accessed 24 October 2004].
- Bai Zhang-Zhen, Tang Jun-Man, Ni Jing, Zheng Tian-Tian, Zhou Yang, Sun Dao-Yang, *et al.* Comprehensive metabolite profile of multi-bioactive extract from tree peony (*Paeonia ostii* and *Paeonia rockii*) fruits based on MS/MS molecular networking. *Food Res Int.* 2021;148:110609. <https://doi.org/10.1016/j.foodres.2021.110609>
- Chen Wenbin, Tu Xijuan, Wu Dehui, Gao Zhaosheng, Wu Siyuan, Huang Shaokang. Comparison of the partition efficiencies of multiple phenolic compounds contained in propolis in different modes of acetonitrile–water-based homogenous liquid–liquid extraction. *Molecules.* 2019;24(3):442. <https://doi.org/10.3390/molecules24030442>
- Du Weifeng, Zhu Weihao, Ge Weihong, Li Changyu. Research on the effect of spleen-invigorating and anti-swelling active ingredients in crude and processed coix seed based on spectrum-effects relationship combined with chemometrics. *J Pharm Biomed Anal.* 2021;205:114350. <https://doi.org/10.1016/j.jpba.2021.114350>
- Eke Rita, Ejiofor Emmanuel, Oyedemi Sunday, Onoja Samuel, Omeh Ndukaku. Evaluation of nutritional composition of *Citrullus lanatus* Linn. (watermelon) seed and biochemical assessment of the seed oil in rats. *J Food Biochem.* 2021;45(6):e13763. <https://doi.org/10.1111/jfbc.13763>
- El-Demerdash Fatma M, El-Sayed Raghda A, Abdel-Daim Mohamed M. *Rosmarinus officinalis* essential oil modulates renal toxicity and oxidative stress induced by potassium dichromate in rats. *J Trace Elem Med Biol.* 2021;67:126791. <https://doi.org/10.1016/j.jtemb.2021.126791>
- Esteki M, Shahsavari Z, Simal-Gandara J. Food identification by high performance liquid chromatography fingerprinting and mathematical processing. *Food Res Int.* 2019;122: 303–17. <https://doi.org/10.1016/j.foodres.2019.04.025>
- Fernández-Pachón Ma Soledad, Villano Débora, Troncoso Ana Ma, García-Parrilla Ma Carmen. [Review of the different methods for the evaluation of the in vitro antioxidant activity of wine and study of in vivo effects]. *Arch Latinoam Nutr.* 2006;56(2):110–22.
- Food and Drug Administration. Botanical Drug Development Guidance for Industry, <https://www.fda.gov/media/93113>; 2016 [Accessed December 2016].
- Gao Yuye, Yu Xie-An, Wang Bing, Yin Guo, Wang Jue, Wang Tiejie, *et al.* Based on multi-activity integrated strategy to screening, characterization and quantification of bioactive compounds from red wine. *Molecules.* 2021;26(21):6750. <https://doi.org/10.3390/molecules26216750>
- Haunschild Robin, Marx Werner. 2022. On health effects of resveratrol in wine. *Int J Environ Res Public Health.* 2022;19(5):3110. <https://doi.org/10.3390/ijerph19053110>
- Huang Yin, Tian Yuan, Zhang Zunjian, Peng Can. A HILIC-MS/MS method for the simultaneous determination of seven organic acids in rat urine as biomarkers of exposure to realgar. *J Chromatogr B Analyt Technol Biomed Life Sci.* 2012;905:37–42. <https://doi.org/10.1016/j.jchromb.2012.07.038>
- Kong Chang-Suk, Kim Jung-Ae, Qian Zhong-Ji, Kim You Ah, Lee Jung Im., Kim Se-Kwon, *et al.* Protective effect of isorhamnetin 3-O-beta-D-glucopyranoside from *Salicornia herbacea* against oxidation-induced cell damage. *Food Chem Toxicol.* 2009;47(8):1914–20. <https://doi.org/10.1016/j.fct.2009.05.002>

- Lavigne Elodie Gras, Cavagnino Andrea, Steinschneider Rémy, Breton Lionel, Baraibar Martin A, Jäger Sibylle. 2022. Oxidative damage prevention in human skin and sensory neurons by a salicylic acid derivative. *Free Radic Biol Med*. 2022;181:98–104. <https://doi.org/10.1016/j.freeradbiomed.2022.01.029>
- Ma Fengwei, Gong Xiaojian, Zhou Xin, Zhao Yang, Li Menglin. An UHPLC-MS/MS method for simultaneous quantification of gallic acid and protocatechuic acid in rat plasma after oral administration of *Polygonum capitatum* extract and its application to pharmacokinetics. *J Ethnopharmacol*. 2015;162:377–83. <https://doi.org/10.1016/j.jep.2014.12.044>
- Manjunatha S, Shaik Althaf Hussain, Maruthi Prasad E, Al Omar Suliman Yousef, Mohammad Altaf, Kodidhela Lakshmi Devi. Combined cardio-protective ability of syringic acid and resveratrol against isoproterenol induced cardio-toxicity in rats via attenuating NF- $\kappa$ B and TNF- $\alpha$  pathways. *Sci Rep*. 2020;10(1):3426. <https://doi.org/10.1038/s41598-020-59925-0>
- Navajas-Porras Beatriz, Pérez-Burillo Sergio, Valverde-Moya Álvaro Jesús, Hinojosa-Nogueira Daniel, Pastoriza Silvia, Rufián-Henares José Ángel. Effect of cooking methods on the antioxidant capacity of plant foods submitted to in vitro digestion-fermentation. *Antioxidants (Basel)*. 2020;9(12):1312. <https://doi.org/10.3390/antiox9121312>
- Plumb Jenny, Durazzo Alessandra, Lucarini Massimo, Camilli Emanuela, Turrini Aida, Marletta Luisa, et al. Extractable and non-extractable antioxidants composition in the eBASIS database: A key tool for dietary assessment in human health and disease research. *Nutrients*. 2020;12(11):3405. <https://doi.org/10.3390/nu12113405>
- Rao Si-Wei, Duan Yuan-Yuan, Pang Han-Qing, Xu Shao-Hua, Hu Shou-Qian, Cheng Ke-Guang, et al. Spectrum-effect relationship analysis of bioactive compounds in *Zanthoxylum nitidum* (Roxb.) DC by ultra-high performance liquid chromatography mass spectrometry coupled with comprehensive filtering approaches. *Front Pharmacol*. 2022;13:794277. <https://doi.org/10.3389/fphar.2022.794277>
- Sohrabi Farzaneh, Dianat Mahin, Badavi Mohammad, Radan Maryam, Mard Seyyed Ali. Gallic acid suppresses inflammation and oxidative stress through modulating Nrf2-HO-1-NF- $\kappa$ B signaling pathways in elastase-induced emphysema in rats. *Environ Sci Pollut Res Int*. 2021;28(40):56822–34. <https://doi.org/10.1007/s11356-021-14513-1>
- Somade Oluwatobi T, Adeyi Olubisi E, Ajayi Babajide O, Asunde Osiro O, Iloh Precious D, Adesanya Adedayo A, et al. Syringic and ascorbic acids prevent NDMA-induced pulmonary fibrogenesis, inflammation, apoptosis, and oxidative stress through the regulation of PI3K-Akt/PKB-mTOR-PTEN signaling pathway. *Metabol Open*. 2022;14:100179. <https://doi.org/10.1016/j.metop.2022.100179>
- Spagnol Caroline Magnani, Assis Renata Pires, Brunetti Iguatemy Lourenço, Isaac Vera Lucia Borges, Salgado Hérica Regina Nunes, Corrêa Marcos Antonio. In vitro methods to determine the antioxidant activity of caffeic acid. *Spectrochim Acta A Mol Biomol Spectrosc*. 2019;219:358–66. <https://doi.org/10.1016/j.saa.2019.04.025>
- Svoboda Pavel, Vlčková Hana, Nováková Lucie. Development and validation of UHPLC-MS/MS method for determination of eight naturally occurring catechin derivatives in various tea samples and the role of matrix effects. *J Pharm Biomed Anal*. 2015;114:62–70. <https://doi.org/10.1016/j.jpba.2015.04.026>
- Tkacz Karolina, Wojdyło Aneta, Turkiewicz Igor P, Ferreres Federico, Moreno Diego A, Nowicka Paulina. UPLC-PDA-Q/TOF-MS profiling of phenolic and carotenoid compounds and their influence on anticholinergic potential for AChE and BuChE inhibition and on-line antioxidant activity of selected *Hippophaë rhamnoides* L. cultivars. *Food Chem*. 2020;309:125766. <https://doi.org/10.1016/j.foodchem.2019.125766>
- Wang Yanan, Wu Haoshuang, Zhou Zhongyi, Maitz Manfred F, Liu Kunpeng, Zhang Bo, et al. A thrombin-triggered self-regulating anticoagulant strategy combined with anti-inflammatory capacity for blood-contacting implants. *Sci Adv*. 2022;8(9):eabm3378. <https://doi.org/10.1126/sciadv.abm3378>
- World Health Organization. Program on traditional medicine. Guidelines for the assessment of herbal medicines. World Health Organization, <https://apps.who.int/iris/handle/10665/58865>; 1991 [Accessed 13 July 1991].
- Xu Nan, Li Mingchen, Wang Ping, Wang Shuling, Shi Haiyan. Spectrum-effect relationship between antioxidant and anti-inflammatory effects of Banxia Baizhu Tianma decoction: An identification method of active substances with endothelial cell protective effect. *Front Pharmacol*. 2022;13:823341. <https://doi.org/10.3389/fphar.2022.823341>
- Yan Linlin, Yin Peipei, Ma Chao, Liu Yujun. Method development and validation for pharmacokinetic and tissue distributions of ellagic acid using ultrahigh performance liquid chromatography-tandem mass spectrometry (UPLC-MS/MS). *Molecules*. 2014;19(11):18923–35. <https://doi.org/10.3390/molecules191118923>
- Yang Lanping, Xie Xiuman, Zhang Jing, Sun Guoxiang. Microemulsion electrokinetic chromatography in combination with chemometric methods to evaluate the holistic quality consistency and predict the antioxidant activity of *Ixeris sonchifolia* (Bunge) Hance injection. *PLoS One*. 2016;11(6):e0157601. <https://doi.org/10.1371/journal.pone.0157601>
- Zarubina IV, Lukk MV, Shabanov PD. Antihypoxic and antioxidant effects of exogenous succinic acid and aminothiols succinate-containing antihypoxants. *Bull Exp Biol Med*. 2012;153(3):336–9. <https://doi.org/10.1007/s10517-012-1709-5>
- Zhang Xian-Fei, Chen Juan, Yang Jun-Li, Shi Yan-Ping. UPLC-MS/MS analysis for antioxidant components of *Lycii fructus* based on spectrum-effect relationship. *Talanta*. 2018;180:389–95. <https://doi.org/10.1016/j.talanta.2017.12.078>
- Zhang Xiangyu, Wang Shilan, Wu Yujun, Liu Xiaoyi, Wang Junjun, Han Dandan. Ellagic acid alleviates diquat-induced jejunum oxidative stress in C57BL/6 mice through activating Nrf2 mediated signaling pathway. *Nutrients*. 2022;14(5):1103. <https://doi.org/10.3390/nu14051103>
- Zhao Yun, Fang Chanlin, Jin Cuiyuan, Bao Zhiwei, Yang Guiling, Jin Yuanxiang. Catechin from green tea had the potential to decrease the chlorpyrifos induced oxidative stress in larval zebrafish (*Danio rerio*). *Pestic Biochem Physiol*. 2022;182:105028. <https://doi.org/10.1016/j.pestbp.2021.105028>